bic symmetry by the occluded template. After 408 hours, only sodalite (lines at −116.2 and −117.0 ppm) remains.

Figure 2B shows solution ^{29}Si NMR spectra of the mother liquor at different reaction times. The ^{29}Si spectrum measured with proton decoupling detects only the unreacted silica. However, when no decoupling is used, lines from 5-coordinate Si (−104.3 ± 0.4 and −105.3 ± 0.3 ppm) become apparent. They are not observed under decoupling because of the negative nuclear Overhauser effect of ^{29}Si (*16*). The intensity of the −105.3-ppm line decreases in the course of the reaction while the intensity of the −104.3-ppm line remains constant, so that their intensity ratio changes from 1:3.5 to 1:1. Silicoglycolate, responsible for the dwindling line, is therefore an intermediate in the synthesis, and we observe a gradual disappearance of 5-coordinate Si. The unchanging line at −104.3 ppm is probably due to some 5-coordinate by-product. Because no other ^{29}Si line is found either in the mother liquor or in the solid product, 5-coordinate Si is clearly a reaction intermediate.

To prove that Na-Si^{V} is indeed an intermediate, we successfully prepared several silicates from crystalline Na-Si^{V} as a starting material. Purely siliceous sodalite was obtained at 190°C from a gel with a composition of Na-Si^{V}:0.3 TBABr:6 H_2O:40 $(CH_2OH)_2$. When no water was present, the product was amorphous. Although the role of water is not completely clear, its presence is essential to break up the 5-coordinate silicate.

Conventional aluminosilicate sodalite was synthesized with Catapal B alumina (70% Al_2O_3) (Vista Chemical Company, Houston, Texas) as the source of aluminum. The molar composition of the gel was Na-Si^{V}:Al_2O_3:40 $(CH_2OH)_2$:0.3 TPABr. The synthetic procedure was the same as above except that H_2O came from Catapal B alumina, which contains 30% water.

The molecular sieve silicalite can be prepared from Na-Si^{V} in the absence of ethylene glycol and only water as solvent, from a gel with a molar composition of Na-Si^{V}:40 H_2O:0.3 TPABr. Silicoglycolate and then TPABr were stirred in water for 10 min, and then the mixture was heated in an autoclave under autogeneous pressure for 3 days. At temperatures between 200° and 240°C, the product was pure α quartz; at 180°C, it was silicalite with a small amount (3% by weight) of α quartz; and at 170°C, it was pure and highly crystalline silicalite.

REFERENCES AND NOTES

1. F. Liebau, *Structural Chemistry of Silicates* (Springer, Berlin, 1985).
2. H. Bartels and H. Erlenmeyer, *Helv. Chim. Acta* **47**, 7 (1964).
3. R. Bach and H. Sticher, *Experientia* **22**, 515 (1966); *Schweiz. Landwirtsch. Forsch.* **2**, 139 (1963).
4. J. F. Stebbins, *Nature* **351**, 638 (1991).
5. R. R. Holmes, *Chem. Rev.* **90**, 17 (1990), and references therein.
6. R. J. P. Corriu and J. C. Young, in *The Chemistry of Organic Silicon Compounds*, S. Patai and Z. Rappaport, Eds. (Wiley, Chichester, UK, 1989), chap. 20, and references therein.
7. S. N. Tandura, M. G. Voronkov, N. V. Alekseev, *Top. Curr. Chem.* **131**, 99 (1986).
8. R. M. Laine *et al., Nature* **353**, 642 (1991).
9. K. Y. Blohoviac, R. M. Laine, T. R. Robinson, M. L. Hoppe, J. Kampf, in *Inorganic and Organometallic Polymers with Special Properties*, R. M. Laine, Ed. (Kluwer, Dordrecht, Netherlands, 1992), pp. 99–111.
10. W. Thomson, *Lond. Edinb. Dublin Philos. Mag. J. Sci.* **24**, 503 (1887).
11. W. A. Deer, R. A. Howie, J. Zussman, *An Introduction to the Rock-Forming Minerals* (Longman, London, ed. 2, 1992), pp. 496–502.
12. R. M. Barrer, *Hydrothermal Chemistry of Zeolites* (Academic Press, London, 1982).
13. D. M. Bibby and P. Dale, *Nature* **317**, 157 (1985).
14. J. W. Richardson, J. J. Pluth, J. V. Smith, W. J. Dytrych, D. M. Bibby, *J. Phys. Chem.* **92**, 243 (1988).
15. B. Herreros, T. L. Barr, J. Klinowski, *ibid.*, in press.
16. H. Marsmann, *NMR 17: Basic Principles and Progress*, P. Diehl, E. Fluck, R. Kosfeld, Eds. (Springer, Berlin, 1981), pp. 65–235.
17. J. Rocha and J. Klinowski, *J. Magn. Reson.* **90**, 567 (1990).
18. G. Engelhardt and D. Michel, *High-resolution Solid-State NMR of Silicates and Zeolites* (Wiley, Chichester, UK, 1987).

19. We thank G. Engelhardt and R. M. Barrer for comments on the manuscript and Unilever Research, Port Sunlight, for support.

25 October 1993; accepted 17 December 1993

Recent Changes in Atmospheric Carbon Monoxide

Paul C. Novelli,* Ken A. Masarie, Pieter P. Tans, Patricia M. Lang

Measurements of carbon monoxide (CO) in air samples collected from 27 locations between 71°N and 41°S show that atmospheric levels of this gas have decreased worldwide over the past 2 to 5 years. During this period, CO decreased at nearly a constant rate in the high northern latitudes. In contrast, in the tropics an abrupt decrease occurred beginning at the end of 1991. In the Northern Hemisphere, CO decreased at a spatially and temporally averaged rate of 7.3 (±0.9) parts per billion per year (6.1 percent per year) from June 1990 to June 1993, whereas in the Southern Hemisphere, CO decreased 4.2 (±0.5) parts per billion per year (7.0 percent per year). This recent change is opposite a long-term trend of a 1 to 2 percent per year increase inferred from measurements made in the Northern Hemisphere during the past 30 years.

The oxidative chemistry of the troposphere is strongly influenced by levels of CO (*1, 2*). Reaction with the hydroxyl radical (OH) is the primary sink for many gases emitted into the atmosphere, including CO, methane, and the replacements for the chlorofluorocarbons. The largest loss of OH is attributable to the reaction between CO and OH, which is controlled, in part, by CO concentration. Mixing ratios for CO in the troposphere have been reported by a number of laboratories over the past 25 years (*3*), and despite continuing uncertainties regarding absolute accuracies and calibrations, the qualitative distributions of CO are known. The mixing ratios in the background troposphere range from about 45 to 250 parts per billion (ppb). Levels decrease from north to south, are greatest in the late winter and early spring, and decrease during the summer. There is also significant interannual variation in its seasonal cycle, and short-term increases and decreases in CO levels have been observed (*4–6*).

Less well defined are long-term changes in atmospheric CO levels. Comparison of spectroscopic measurements made in 1950–1951 to measurements made in the 1980s suggest that CO levels in the Northern Hemisphere (NH) increased at an average rate of ~1% per year over that period (*5*). In the Southern Hemisphere (SH), continuous measurements made from 1979 to 1987 at Cape Point, South Africa, show no significant trend (*6*). Grab samples of air collected during the 1980s from six locations worldwide indicate a ~1% per year increase (*7*); however, more recent data from these stations suggest a possible decrease in CO (*8*). The CO growth rates, like mixing ratios, surely vary with time and location; thus, global trends may be difficult to determine on the basis of measurements from a few isolated sites. Here we discuss recent changes in tropospheric CO measured at 27 globally distributed sampling sites in the marine boundary layer (MBL) between June 1990 and June 1993.

Air samples were collected weekly at 10

P. C. Novelli and K. A. Masarie, Cooperative Institute for Research in Environmental Sciences, University of Colorado, Boulder, CO 80309–0449, USA.
P. P. Tans and P. M. Lang, Climate Monitoring and Diagnostics Laboratory, Environmental Research Laboratory, National Oceanic and Atmospheric Administration, 325 Broadway, Boulder, CO 80303, USA.

*To whom correspondence should be addressed.

fixed locations between 71°N and 41°S and about once every 3 weeks from a ship at 17 latitudes from 45°N to 35°S in the Pacific Ocean (*9*) (Fig. 1). The samples were shipped to Boulder, Colorado, and within 1 to 6 weeks of collection were analyzed for CO by gas chromatography followed by mercuric oxide reduction. All measurements were referenced to the Climate Monitoring and Diagnostics Laboratory (CMDL) CO reference scale (*10*); mixing ratios are reported in parts per billion by mole fraction. Evaluation of standard stabilities, instrument response characteristics, and calibration procedures used in this study have been presented in detail elsewhere (*11*).

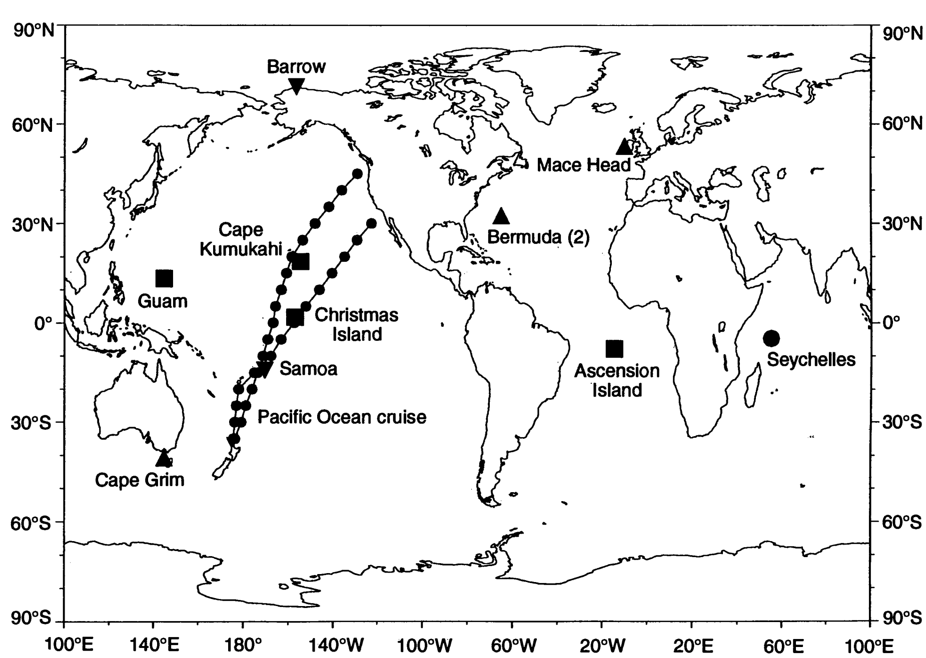

Fig. 1. Locations of sample collection. Sites first sampled in 1988 are represented by (▼), in 1989 by (■), in 1990 by (●), and in 1991 by (▲). The Pacific cruise sites were located at intervals of 5° and were collected aboard the M.V. *Wellington Star*. The northward and southward cruise tracks are connected by straight lines.

The trend and seasonal cycle of CO at each site was approximated by fitting a polynomial function and four harmonics to the data (Fig. 2)

$$f(t) = a_1 + a_2t + a_3t^2 + \dots + a_{np}t^{np-1} + \sum_{i=1}^{4}[a_{2i+np-1}\sin(2\pi it) + a_{2i+np}\cos(2\pi it)] \qquad (1)$$

where np is the number of polynomial terms, t is the time in years, and a_i are defined by the fit. Average seasonal variation is represented by the harmonics, and the trend is determined from the polynomial. The residuals (the difference between the curve and the measured values) were smoothed with a fast Fourier transform algorithm and two different low-pass filters. One filter captured variations from the seasonal cycle, and the other described variations only in the long-term trend. The final fit—consisting of the sum of the polynomials, the harmonics, and the filtered residuals (*12*)—represented background CO mixing ratios for each site. The trend consisted of the polynomial terms and residuals filtered by the second low-pass filter. The 27 time series were spatially averaged over the period of June 1990 to June 1993 with a meridional curve fit to each 2-week interval (*13*) (Fig. 3) or with a simple triangulation approach (*14*).

The smoothed data show (i) there was strong seasonal cycle of CO in the NH, (ii) CO mixing ratios ranged from about 230 ppb in the northern winter to 45 ppb in the southern summer, and (iii) the latitudinal gradient changed seasonally. We used the spatially smoothed CO values to calculate average CO time series for latitude bins representing equal segments of the Earth's surface: the four semihemispheres, the two hemispheres, and a global average. The average rate of change over the time series was taken as a_2t from Eq. 1. Errors were estimated with bootstrap techniques (*15*, *16*) by randomly picking sites (with restitution) from the 27 sites. There was no significant difference between rates determined by the two different smoothing routines.

The data show that atmospheric CO levels have decreased over the past few years. The rate of change for the 27 sites ranged from −7.8 ppb of CO per year to −1.5 ppb per year. Levels decreased in all seasons of the year. Measurements made at four sites with altitudes greater than 2500 m, which were not used in the global averages, exhibited rates of CO decrease similar to those in the MBL (*17*). We determined trends (Fig. 4) using the zonally averaged mixing ratios presented in Fig. 3. Between June 1990 and June 1993, the globally averaged level of CO decreased 5.9 (±0.55) ppb year^{-1}. The global average CO mixing ratio was 93 ppb in 1991 and 87 ppb in 1992. Whereas CO levels decreased most in the high NH (30° to 90°N, 7.7 ± 1.2 ppb year^{-1}) and least in the low SH (0° to 30°S, 3.7 ± 0.3 ppb year^{-1}), the rates of change relative to the average mixing ratios of the respective semihemispheres were the same (−5.6% year^{-1}). The rate of CO decrease in the NH (7.3 ± 0.92 ppb year^{-1}) was about 75% greater than that in the SH (4.2 ± 0.47 ppb year^{-1}), but again, the relative rate of change was quite similar (−6.1 ± 0.8% per year in the NH, −6.9 ± 0.7% per year in the SH). The greatest rates of CO decrease were observed from the end of 1991 through 1993 at all latitudes, particularly in the tropics.

The global CO budget is dominated by four sources: fossil fuel combustion and industrial emissions, biomass burning, oxidation of CH$_4$, and oxidation of nonmethane hydrocarbons (NMHC). Each term has an estimated source strength between 400 and 1000 Tg (1 Tg = 10^{12} g) of CO per year. Reaction with OH (CO + OH → CO$_2$ + H) accounts for 90 to 95% of the sink (*1*, *18*). An increasing trend in atmospheric CO results from an excess of the sources relative to sinks, whereas a negative growth rate results from an excess of sinks over sources. In consideration of the earlier evidence for a long-term increase in atmospheric CO levels, our data imply that the balance of sources and sinks has recently changed. To estimate the effect of changing CO sources and sinks on atmospheric mixing ratios, we describe the steady-state CO level as

$$\frac{d[\mathrm{CO}]_\mathrm{H}}{dt} = \Sigma S_i - K_\mathrm{OH}[\mathrm{CO}]_\mathrm{H} \qquad (2)$$

where brackets represent concentration, the subscript H indicates the hemisphere, S_i is the rate of CO emission from source i, and K_OH[CO] is the loss rate of CO by reaction with OH. We assume a steady state over 1 year or more (much longer than the CO lifetime, which is about 2 months), which implies that $[\mathrm{CO}]_\mathrm{H} = \Sigma S_i/K_\mathrm{OH}$. We take the differential of this and rearrange to give

$$\frac{d[\mathrm{CO}]}{[\mathrm{CO}]} = \frac{\Sigma dS_i}{\Sigma S_i} - \frac{d[\mathrm{OH}]}{[\mathrm{OH}]} \qquad (3)$$

Oxidation of CO by reaction with OH is the single largest term in the CO budget.

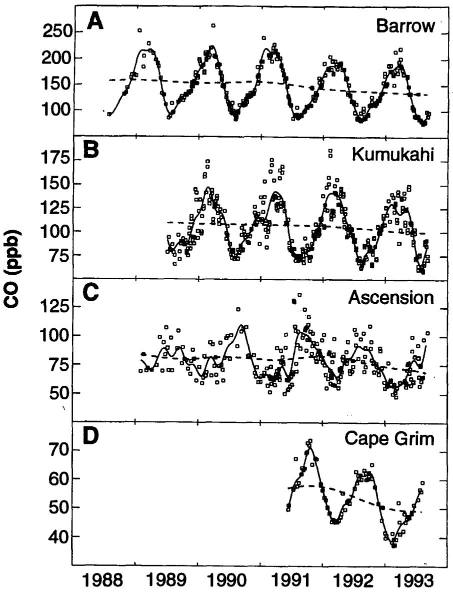

Fig. 2. The CO time series from (**A**) Barrow, Alaska; (**B**) Cape Kumukahi, Hawaii; (**C**) Ascension Island; and (**D**) Cape Grim, Tasmania. The trend (dashed line) and smoothed curve (solid line) were calculated with Eq. 1.

Prinn *et al.* (*19*) used a 12-year record of methylchloroform measurements to calculate global OH distributions and a globally averaged rate of change of +1.0 ± 0.8% per year. Using Eq. 3 with $d\Sigma S_i/\Sigma S_i = 0$, $[\mathrm{CO}]_{\mathrm{NH}} = 120$ ppb, $[\mathrm{CO}]_{\mathrm{SH}} = 60$ ppb, and $d[\mathrm{OH}]/[\mathrm{OH}] = +1.0 \pm 0.8\%$ per year, we predict that increased oxidation can account for CO decreases at rates ranging from 1.2 ± 1.0 ppb year^{-1} in the NH to 0.6 ± 0.5 ppb year^{-1} in the SH.

The oxidation of methane through reaction with OH accounts for 20 to 30% of the total global CO source and can be described as $S_{\mathrm{CH_4}} = 0.9\ k_{\mathrm{CH_4}}[\mathrm{CH_4}][\mathrm{OH}]$, where the yield of CO from CH_4 oxidation is 90%. Relative changes in this CO source are described by $dS_{\mathrm{CH_4}}/S_{\mathrm{CH_4}} = d[\mathrm{CH_4}]/[\mathrm{CH_4}] + d[\mathrm{OH}]/[\mathrm{OH}]$. Again we assume that [OH] increased 1.0 ± 0.8% per year, $[\mathrm{CH_4}]$ increased 0.5% per year, methane oxidation comprised 23% of the total CO source in the NH and 44% in the SH, and average hemispheric CO concentrations are as given above. We estimate that increased methane oxidation can account for CO rising about equally in both hemispheres at 0.4 ± 0.2 ppb year^{-1}.

Before the United States and the European Economic Community severely tightened pollution controls in the mid-1970s and early 1980s, respectively, emissions of CO from transportation sources in Europe and North America accounted for slightly more than 50% of the total CO from fossil fuel use (*1*). Bakwin *et al.* (*20*) modeled changes in tropospheric CO levels resulting from improved emission controls. They predicted an average decrease of 0.9 (±0.5) ppb year^{-1} in the NH over the period of 1976 to 1990.

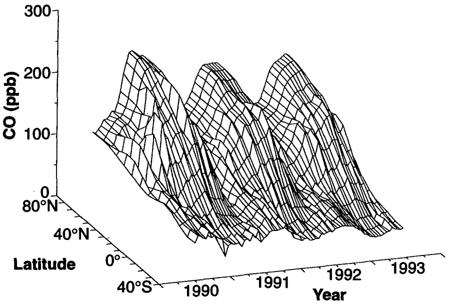

Fig. 3. Three-dimensional representation of the global distribution of atmospheric CO generated with Eq. 1 and meridional smoothing. Data from 27 sites in the MBL were used. Global data begins June 1990, although some sites were sampled earlier. Grid spacing is 14 days by 10° latitude. The distribution assumes no longitudinal variations; however, data from different longitudes were averaged when more than one site in a latitudinal band was represented.

The net effect of these changes in sources and sinks is a predicted decrease in atmospheric CO levels at rates of 1.7 ± 1.3 ppb year^{-1} in the NH and 0.2 ± 0.3 ppb year^{-1} in the SH. Even considering the large uncertainties, these rates are much smaller than those observed. We may have underestimated changes in CO production from fossil fuel combustion, particularly as emissions from the former Soviet Union have decreased recently because of economic contraction. However, it is highly unlikely that the decrease in atmospheric CO can be explained completely by changes in fossil fuel. Using Eq. 3 with $d[\mathrm{CO}]/[\mathrm{CO}] = -6.5\%$ per year; $S_i = 20\%$ (fossil fuel contribution to the total global source), and $d[\mathrm{OH}]/[\mathrm{OH}] = 0$, we find that CO from fossil fuel combustion must have decreased by an implausible 30% per year.

It is also possible that OH has increased more than 1 to 2% per year over the past 2 years. The eruption of Mount Pinatubo in June 1991 may be responsible for a recent decrease of stratospheric O_3 levels (*21*), which could result in greater ultraviolet (UV) radiation reaching the troposphere. If UV radiation increased, we would expect an increase in the photolysis of tropospheric O_3 and an increase in OH levels (*22*). In the background atmosphere, increasing OH levels could lead to even greater decreases in CO levels because of a positive feedback between increasing OH and decreasing CO. Our data show that the greatest rate of CO decrease began in late 1991 and early 1992, the timing of which corresponds to the Pinatubo eruption. The rate of CO decrease relative to the average mixing ratio is similar in both hemispheres, suggesting that the decline in CO may be proportional to its mixing ratio. However, there was not a dramatic decrease in summer CO levels in 1992 or 1993 as would be expected if CO oxidation increased with greater UV radiation.

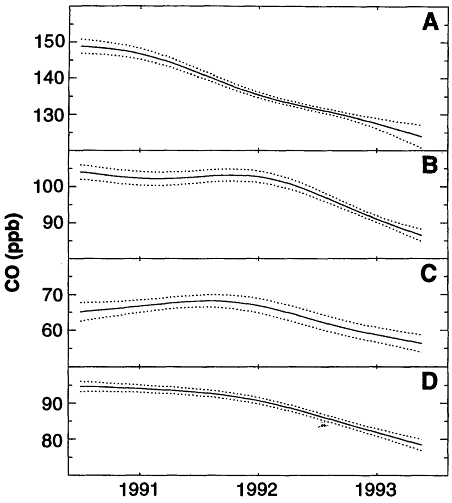

Fig. 4. The CO change from 1990 to 1993. (**A**) High NH (30° to 90°N), (**B**) low NH (0° to 30°N), (**C**) low SH (0° to 30°S), and (**D**) global average. The dashed lines represent 1σ confidence intervals.

Two additional sources of CO must also be considered: biomass burning and the oxidation of naturally emitted NMHCs. Each contributes about 25% to the global CO source. Possible changes in emissions of carbon gases from these processes are uncertain (*23*). However, emissions of CO from biomass burning affect CO distribution in the tropics, and this source is highly variable from year to year (*24*). Interannual variations of CO at low latitudes may be caused in part by variations in biomass burning.

The decrease in atmospheric CO is most likely attributable to a combination of changes in sources and sinks. Further measurements will confirm if this downward trend continues. If so, it will signify an important change in tropospheric oxidation processes. Independent of future trends, these recent changes are significant because they have at least temporarily lowered the global background level of CO.

REFERENCES AND NOTES

1. J. A. Logan, M. J. Prather, S. C. Wofsy, M. B. McElroy, *J. Geophys. Res.* **86**, 7210 (1981).
2. A. M. Thompson, *Science* **256**, 1157 (1992).
3. P. C. Novelli, L. P. Steele, P. P. Tans, *J. Geophys. Res.* **97**, 20731 (1992), and references therein.
4. World Meteorological Organization, "Scientific Assessment of Ozone Depletion: 1991," *WMO Report No. 25* (1993), pp. 1.25–1.3.
5. R. Zander, Ph. Demoulin, D. H. Ehhalt, U. Schmidt, C. P. Rinsland, *J. Geophys. Res.* **94**, 11021 (1989).
6. E.-G. Brunke, H. E. Scheel, W. Seiler, *Atmos. Environ. A* **24**, 585 (1990).

7. M. A. K. Khalil and R. A. Rasmussen, *Nature* **332**, 242 (1988).
8. ______, in preparation.
9. The Climate Monitoring and Diagnostics Laboratory (CMDL) of the U.S. National Oceanic and Atmospheric Administration (NOAA) operates a global network of sampling sites where air is collected and used to determine the distributions, budgets, and trends of CO_2, CH_4, and CO. Sites are chosen to represent background conditions; that is, to reflect regional-scale processes and not local sources or sinks [T. J. Conway *et al.*, *Tellus Ser. B* **40**, 81 (1988); (*16*)].
10. Two instruments were used for this work, and the instrument response characteristics were described with the use of multiple standards. From July 1988 through December 1990, flask samples were analyzed with an instrument having a linear response over the range of 0 to 1000 ppb of CO (*3*). From January 1991 to June 1993, an instrument with a nonlinear response was used, and a multipoint (seven to nine standards) calibration scheme quantified CO mixing ratios [P. C. Novelli, L. P. Steele, J. W. Elkins, *J. Geophys. Res.* **96**, 13109 (1991)].
11. P. C. Novelli, J. E. Collins Jr., R. C. Myers, G. W. Sachse, H. E. Scheel, *ibid.*, in press. The CMDL calibration procedure is described, and the stabilities of the standards used for both flask sample analysis and calibration of reference gases are reviewed. On the basis of intercomparison of gravimetric standards produced in 1988–1989 and in 1992 and upon intercalibration of working standards, we conclude that the CMDL standard scale has been maintained to a precision of 1% or better. Drift rates in standards were <1% and not significant (2σ).
12. K. W. Thoning, P. P. Tans, W. D. Komhyr, *J. Geophys. Res.* **94**, 8549 (1989). For sites with ≤ 3 years of data, $np = 2$; for those with >3 years, $np = 3$.
13. P. P. Tans, T. J. Conway, T. Nakazawa, *ibid.* **94**, 5151 (1989).
14. We first used a Delaunay triangulation routine to construct a planar set of points and then created a grid using a linear interpolation.
15. P. Diaconis and B. Efron, *Sci. Am.* **248**, 116 (May 1983).
16. L. P. Steele *et al.*, *Nature* **358**, 313 (1992).
17. Air samples were collected weekly at four high-altitude sites: Niwot Ridge, Colorado (40°N,106°W); Qinghai Province, China (36°N,101°E); Mauna Loa, Hawaii (20°N,156°W); and Tenerife, Canary Islands (28°N,6°W).
18. P. Warneck, *Chemistry of the Natural Atmosphere* (Int. Geophys. Ser. 41, Academic Press, San Diego, CA, 1988), pp. 158–170.
19. R. Prinn *et al.*, *J. Geophys. Res.* **97**, 2445 (1992).
20. P. S. Bakwin, P. P. Tans, P. C. Novelli, *Geophys. Res. Lett.*, in press. The authors model changes in CO over the past 14 years using a simple mass-balance approach. Using CO measurements from Barrow, Alaska; Harvard Forest, Massachusetts; the Atlantic arctic; and Zugspitze, Germany, they concluded CO may have decreased at a rate of 0.9 (±0.5) ppb year^{-1} in the NH solely because of changes in emissions. No significant change was predicted in the SH.
21. J. F. Gleason *et al.*, *Science* **260**, 523 (1993).
22. R. C. Schnell *et al.*, *Nature* **351**, 726 (1991); S. Madronich and C. Granier, *Geophys. Res. Lett.* **19**, 465 (1992), and references therein.
23. R. A. Houghton, *Clim. Change* **19**, 99 (1991); P. M. Fearside, N. Leal Jr., F. M. Fernandes, *J. Geophys. Res.* **98**, 16733 (1993). The NMHC emissions may have decreased because of both economic stagnation and a slowing of deforestation; however, few data are available.
24. G. W. Sachse, R. C. Harriss, J. Fishman, G. F. Hill, D. R. Cahoon, *J. Geophys. Res.* **93**, 1422 (1988); J. Fishman, K. Fakhruzzaman, B. Cros, D. Nganga, *Science* **252**, 1693 (1991); R. A. Delmas, P. Loudjani, A. Podaire, J. C. Menaut, in *Global Biomass Burning*, J. S. Levine, Ed. (MIT Press, Cambridge, MA, 1991), pp. 126–132.
25. We thank N. Zhang for sample analysis, W. Coy and R. Martin for instrument development, and the officers of the M.V. *Wellington Star* (Blue Star Line, London) and personnel at the site locations for the collection of samples. K. Thoning developed many of the smoothing algorithms used here. P. Bakwin provided useful discussions. Funding was provided in part by the Radiatively Important Trace Gas Species component of the NOAA Climate and Global Change Program.

29 November 1993; accepted 2 February 1994

Sound Velocities in Dense Hydrogen and the Interior of Jupiter

Thomas S. Duffy, Willem L. Vos,* Chang-sheng Zha, Russell J. Hemley, Ho-kwang Mao

Sound velocities in fluid and crystalline hydrogen were measured under pressure to 24 gigapascals by Brillouin spectroscopy in the diamond anvil cell. The results provide constraints on the intermolecular interactions of dense hydrogen and are used to construct an intermolecular potential consistent with all available data. Fluid perturbation theory calculations with the potential indicate that sound velocities in hydrogen at conditions of the molecular layer of the Jovian planets are lower than previously believed. Jovian models consistent with the present results remain discrepant with recent free oscillation spectra of the planet by 15 percent. The effect of changing interior temperatures, the metallic phase transition depth, and the fraction of high atomic number material on Jovian oscillation frequencies is also investigated with the Brillouin equation of state. The present data place strong constraints on sound velocities in the Jovian molecular layer and provide an improved basis for interpreting possible Jovian oscillations.

The behavior of hydrogen at high pressure is central to a number of fundamental problems in condensed matter and planetary science (*1*). Measurements of the sound velocity of high-density hydrogen provide critical information on the elastic anisotropy, equation of state (EOS), and other thermodynamic properties of this material. This information is particularly important for the construction of accurate models for the interior structure of the giant planets (*2*). Uncertainty in the EOS of hydrogen is the source of the largest uncertainty in current Jovian models (*3*). Recently, the first successful observations of global free oscillations of Jupiter have been reported (*4*). Such measurements could provide a wealth of new information about the Jovian planets, much as helioseismology has revolutionized understanding of the solar interior. Current interpretations of Jovian oscillation spectra suggest a need for major revisions of interior models (*5*). Free oscillation spectra are sensitive to sound velocities that are directly connected to the EOS in the planet's interior. Thus, measurement of sound velocities in dense hydrogen can provide more direct constraints on the seismic structure of the molecular region of the planet.

We have developed a technique for in situ measurements of the elasticity of hydrogen and similar materials to very high pressures in a diamond anvil cell. We combine acoustic velocities measured by Brillouin scattering with the orientation and number of crystals determined by synchrotron x-ray diffraction. Brillouin scattering uses the frequency shift of laser light scattered by thermally generated sound waves to determine acoustic velocities (*6*). In this study, we have overcome a number of restrictions imposed by the diamond cell on the use of Brillouin scattering at high pressure (*7*). Previously, there have been trade-offs between maximum pressure, number of crystallographic orientations probed, and the ability to separate the acoustic velocity from the refractive index. A complete determination of the elastic properties of anisotropic crystals requires the use of multiple scattering geometries, measurements in many crystallographic directions, and careful characterization of the crystals. The latter is a particular problem for materials that are gases at ambient pressure and whose orientation cannot be controlled when solidified at high pressure in the diamond cell.

The development of single-crystal x-ray diffraction using synchrotron radiation for low atomic number materials has led to significant advances in the understanding of hydrogen and other molecular solids (*8, 9*). Synchrotron x-ray diffraction measurements on H_2 (*8, 10, 11*) tightly constrain the EOS between 5.4 and 42 GPa at room temperature. This EOS is consistent with data obtained by other methods (*12*). In this study, we use a pair potential model

---

Geophysical Laboratory and Center for High-Pressure Research, Carnegie Institution of Washington, 5251 Broad Branch Road, NW, Washington, DC 20015, USA.

*Present address: van der Waals–Zeeman Laboratorium, Universiteit van Amsterdam, 1018 XE Amsterdam, The Netherlands.